

## Doping Dependence of the Mass Enhancement in $(\text{Pb, Bi})_2\text{Sr}_2\text{CaCu}_2\text{O}_8$ at the Antinodal Point in the Superconducting and Normal States

T. K. Kim,<sup>1</sup> A. A. Kordyuk,<sup>1,3</sup> S. V. Borisenko,<sup>1</sup> A. Koitzsch,<sup>1</sup> M. Knupfer,<sup>1</sup> H. Berger,<sup>2</sup> and J. Fink<sup>1</sup>

<sup>1</sup>*Leibniz-Institute for Solid State and Materials Research Dresden, P.O.Box 270116, D-01171 Dresden, Germany*

<sup>2</sup>*Institut de Physique de la Matière Complex, Ecole Polytechnique Fédérale de Lausanne, CH-1015 Lausanne, Switzerland*

<sup>3</sup>*Institute for Metal Physics of the National Academy of Sciences of Ukraine, 03142 Kyiv, Ukraine*

(Received 20 March 2003; published 14 October 2003)

Angle-resolved photoemission spectroscopy is used to study the mass renormalization of the charge carriers in the high- $T_c$  superconductor  $(\text{Pb, Bi})_2\text{Sr}_2\text{CaCu}_2\text{O}_8$  in the vicinity of the  $(\pi, 0)$  point in the superconducting and the normal states. Using matrix element effects at different photon energies and due to a high momentum and energy resolution the bonding and the antibonding bands could be separated in the whole dopant range. A huge coupling to a bosonic collective mode is observed below  $T_c$  for both bands, in particular, for the underdoped case. Above  $T_c$ , a weaker coupling to a continuous spectrum of modes is detected.

DOI: 10.1103/PhysRevLett.91.167002

PACS numbers: 74.25.Jb, 74.72.-h, 79.60.-i

Sixteen years after the discovery of high- $T_c$  superconductors (HTSCs) by Bednorz and Müller [1] the understanding of the electronic transport in these systems is still full of unresolved issues. This holds for both the normal and the superconducting states. In particular, it is not clear whether in these compounds which are close to an antiferromagnetic insulator the interaction between the electrons is large enough to destroy coherence, i.e., the existence of well-defined quasiparticles, and to result in a new state of matter [2]. On the other hand, one can possibly analyze the available experimental data in terms of a strong coupling to bosons such as phonons or spin fluctuations, leading to coherent and incoherent states. Moreover, there are intermediate scenarios [3]. Therefore it is interesting to investigate in which dopant and temperature range coherent states are present.

Traditional angle-resolved photoemission spectroscopy (ARPES) has been an important experimental probe to map out the band structure of solids. Recent improvements of the energy and the momentum resolution opened the possibility to study the many-body properties of solids. The deviation from the independent particle dispersion close to the Fermi level gives information on the renormalization of bands or on the enhanced effective mass. The width of the peaks reflects the scattering rate or the inverse lifetime of the photohole which should behave in a similar way as the charge carriers in a  $p$ -type doped HTSC. Both the mass renormalization and the finite width of the spectral weight are normally described in terms of the real and the imaginary part of the self-energy  $\Sigma$ , respectively.

Numerous ARPES studies on HTSCs [4,5] have shown that the renormalization is strongly momentum dependent; i.e., it is a function of the position on the Fermi surface. Up to now there are many ARPES studies along the nodal direction [the  $\Gamma - (\pi, \pi)$  line] where in the superconducting state no gap is opened. All these studies

indicate that there is a mass renormalization  $m^*/m = 1 + \lambda$  at the Fermi level by a factor of about 2 corresponding to a coupling constant  $\lambda$  of about 1. The renormalization extends to an energy of about 70 meV below the Fermi level indicated by a kink in the dispersion. Currently there is no consensus on the origin of this renormalization. Coupling to collective bosonic modes such as phonons or spin fluctuations is discussed.

At the antinodal point [the  $(\pi, 0) - (\pi, \pi)$  Fermi surface crossing] where the superconducting gap has a maximum, only a few experimental studies exist [4–8]. Moreover, the situation is more complicated by the fact that in  $\text{Bi}_2\text{Sr}_2\text{CaCu}_2\text{O}_8$  (Bi2212), the so-called bilayer splitting into a bonding ( $B$ ) and an antibonding ( $A$ ) band appears in this region of the Brillouin zone due to an interaction between two adjacent  $\text{CuO}_2$  layers. This bilayer splitting could not be resolved in many previous low resolution experiments and therefore the existence of coherent states could be overlooked. On the other hand, the investigation of bilayer systems offers the unique possibility to study the interaction of  $\text{CuO}_2$  layers which is of extreme importance for the understanding of the mechanism of high- $T_c$  superconductivity, since  $T_c$  increases with the number of interacting layers up to three and then decreases again.

In this Letter we present high resolution ARPES data of Bi2212 around the  $(\pi, 0)$  point for the whole dopant range from the overdoped (OD) via optimally doped (OP) to underdoped (UD) samples. Contrary to previous experiments [6], we find dispersing renormalized bands not only in the superconducting state but also in the normal state in the whole dopant range, even for UD samples. Since we used the photon energy dependence of the excitations from the  $B$  and  $A$  bands we could determine the respective renormalization of both bands. It turned out that above  $T_c$  the renormalization is rather isotropic and weaker than in the superconducting state. No kink and no

specific energy scale could be detected. In the superconducting state the renormalization due to a coupling to a collective bosonic mode is very strong and increases with decreasing dopant concentration. The results are in contrast to the traditional view, in which due to correlation effects in the normal state of UD samples no dispersing states exist and in the superconducting state the number of coherent states are expected to increase. Thus, the present results indicate a continuous transition from a more conventional metal to a strange metal with a small number of coherent states and not a transition into a new state of matter when going from the OD to the UD region.

The ARPES experiments were carried out at the BESSY synchrotron radiation facility using the U125/1-PGM beam line and a SCIENTA SES100 analyzer. Spectra were taken with various photon energies ranging from 17 to 65 eV. The total energy resolution ranged from 8 meV (FWHM) at photon energies  $h\nu = 17\text{--}25$  eV to 22.5 meV at  $h\nu = 65$  eV. The momentum resolution was set to  $0.01 \text{ \AA}^{-1}$  parallel to the  $(\pi, 0) - (\pi, \pi)$  direction and  $0.02 \text{ \AA}^{-1}$  parallel to the  $\Gamma - (\pi, 0)$  direction. Here we focus on spectra taken with photon energies of 38 and 50 eV (or 55 eV) to discriminate between  $B$  and  $A$  bands. The polarization of the radiation was along the  $\Gamma - (\pi, 0)$  direction. Measurements have been performed on  $(1 \times 5)$  superstructure-free Pb-Bi2212 single crystals ranging from OD (OD69,  $T_c = 69$  K) via OP (OP89K,  $T_c = 89$  K) to UD (UD77,  $T_c = 77$  K) samples. The dopant concentration was calculated from the empirical equation of  $T_c$  versus the dopant concentration [9].

In Fig. 1 we show a collection of data for wave vectors close to the  $(\pi, \pi) - (\pi, -\pi)$  line, centered around the  $(\pi, 0)$  point. As shown previously [8,10] and supported by theoretical calculations [11], due to matrix element effects the data taken with  $h\nu = 38$  eV represent mainly the  $B$  band with some contributions from the antibonding band while the data taken with  $h\nu = 50$  (or 55) eV have almost pure  $A$  character. The subtraction of the latter from the  $h\nu = 38$  eV data represents almost the pure  $B$  bands. This was performed by scaling the  $h\nu = 50$  eV spectral weight in such a way that at the  $(\pi, 0)$  point no negative intensity occurs. Using this procedure one clearly recognizes that in the whole doping range and even in the UD samples the  $B$  and the  $A$  band can be well separated.

In the superconducting state these data show strong changes upon reducing the dopant concentration: the  $B$  and most clearly seen the  $A$  band moves further and further below the Fermi level and the renormalization strongly increases as indicated by the appearance of a flat dispersion below the gap energy. At  $\sim 70$  meV for the  $B$  band a kink and a reduction of spectral weight is observed, both increasing with decreasing dopant concentration.

In Fig. 2 we show on an enlarged scale data for the  $B$  and  $A$  band of the UD77 sample. Also included are dispersions derived from constant energy scans or momen-

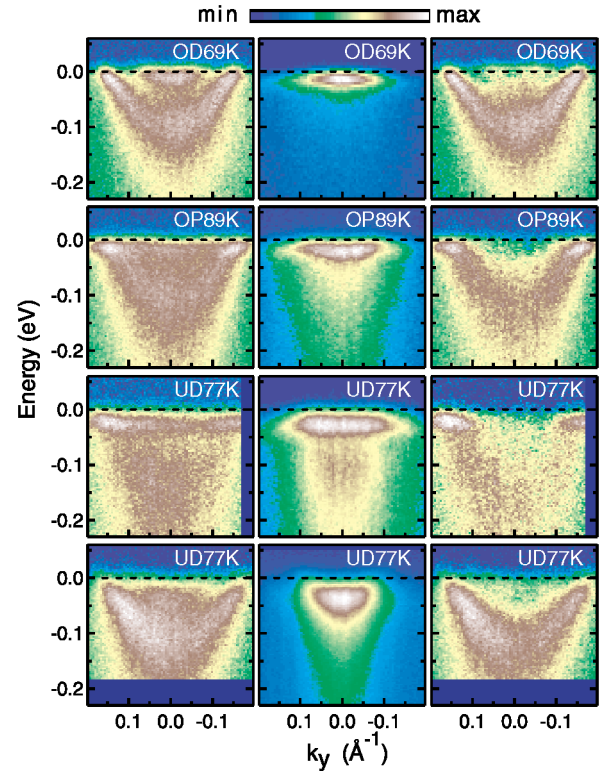


FIG. 1 (color). ARPES intensity plots as a function of energy and wave vectors along the  $(\pi, \pi) - (\pi, -\pi)$  direction of overdoped (OD), optimally doped (OP), and underdoped (UD) Pb-Bi2212 superconductors taken at  $T = 30$  K (upper three rows). Zero corresponds to the  $(\pi, 0)$  point. Bottom row: data for an UD sample taken at  $T = 120$  K. Left column: data taken with a photon energy  $h\nu = 38$  eV, at which the signal from the bonding band is maximal. Middle column: data taken at  $h\nu = 50$  eV (or 55 eV), where the signal from the antibonding band is dominant. Right column: subtraction of the latter from the former yielding the spectral weight of the bonding band (see text for details).

tum distribution curves (MDCs) in red for the  $B$  band and from constant momentum scans or energy distribution curves (EDCs) in blue for both bands. As previously discussed [5,7] the EDC and the MDC dispersions are quite different for weakly dispersing states, i.e., in the superconducting state, while they are similar in the normal state. Below  $T_c$  the EDC derived dispersion shows the typical BCS-type backdispersion due to particle-hole mixing. At 120 K a pseudogap is observed and there is no observable backdispersion. This could explain the absence of a coherent peak in the tunneling spectroscopy data in the pseudogap regime [12].

The EDC depicted in Fig. 2, which was measured in the superconducting state at  $k_F$  of the  $B$  band, is typical of a strong coupling of the charge carriers to a bosonic mode [4,5,7]. For this sample, the dip energy,  $E_D = \Delta + E_M$ , occurs at 70 meV which, with a superconducting gap  $\Delta = 30$  meV, corresponds to a mode energy  $E_M$  of 40 meV [13]. Then the dispersion  $E(k)$  in the vicinity of the

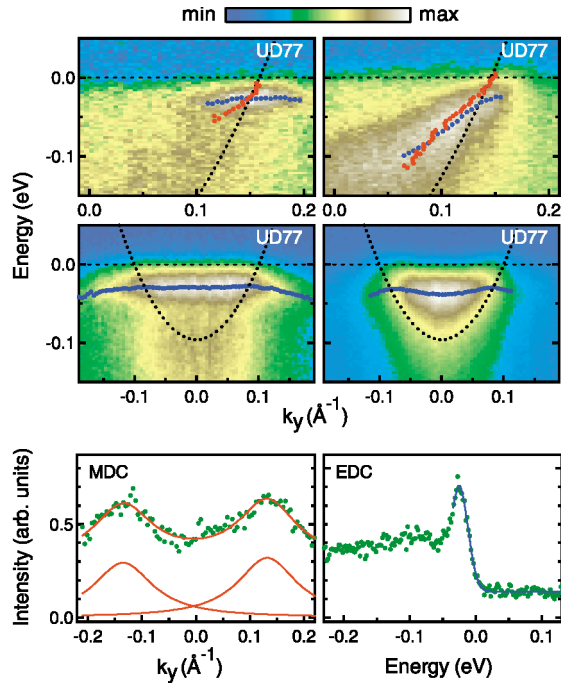


FIG. 2 (color). Top row: dispersion of the bonding band near the antinodal point in an underdoped Pb-Bi2212 sample at  $T = 30$  K (left) and at  $T = 120$  K (right) as derived from EDCs (blue points) and MDCs (red points) together with the bare electron dispersion (black points). Middle row: the same data for the antibonding band. Bottom row: MDCs (left panel) at 30 meV and EDCs (right panel) of the bonding band at  $k_F$  including fits to obtain the maximum.

gap can be approximated by the expression  $E(k) = (\epsilon_k^2 + \Delta^2)^{1/2}$  where  $\epsilon_k$  is a renormalized band dispersion which is approximated by a linear dispersion  $\epsilon_k = v_F^b(k - k_F)/(1 + \lambda)$  where  $v_F^b$  is the Fermi velocity of the *bare* particles and  $k_F$  is the Fermi wave vector [14]. The bare Fermi velocities were taken from a previous evaluation of the Fermi surface and data along the nodal direction in terms of a tight-binding band structure (also shown in Fig. 2) [15]. This band structure is close to that derived from an analysis of the anisotropic plasmon dispersion [16] and to that obtained from local density approximation band structure calculations [17]. In the fits of  $E(k)$  to the EDC dispersions we used three parameters:  $\lambda$ ,  $\Delta$ , and  $k_F$ . The values for  $\lambda$  are presented in Fig. 3 and the  $\Delta$  values are 30, 22, 16 meV for UD, OP, and OD samples, respectively. In OP and OD samples, where steeper dispersions are observed, similar values of  $\lambda$  were also derived from MDC dispersions. For the *A* band reliable values for  $\lambda$  could be obtained only for an UD sample since this band is just crossing the Fermi level.

With decreasing dopant concentration there is a strong increase of the coupling strength from  $\lambda$  of about 3 to huge values of about 8. We emphasize that the increase seems to be continuous and there is no break between the OD and the UD region. For the *A* band in the UD77 sample a similar huge mass renormalization has been

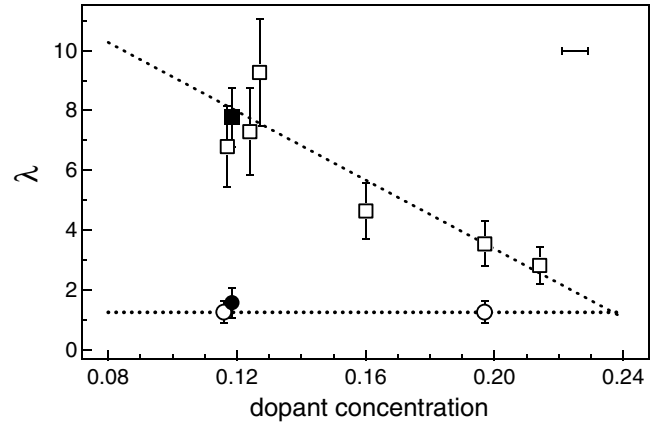


FIG. 3. The coupling strength parameter  $\lambda$  as a function of dopant concentration. Squares: superconducting state; circles: normal state; open (solid) symbols: bonding (antibonding) band. The dashed lines are fits to the data using a straight line. Horizontal bar: experimental error in the dopant concentration.

detected (see Fig. 3). The results for the *A* and the *B* band in the superconducting state can also be summarized in a different way. With decreasing dopant concentration the coherence factor  $Z = 1/(1 + \lambda)$  decreases from 0.25 to 0.1. This means that for UD samples below  $T_c$  only about 1/9 of the spectral weight near  $E_F$  represents coherent states.

Above  $T_c$  we see dispersive states even in UD samples and the renormalization of both bands is strongly reduced (see Fig. 2). There is also no kink in the MDC dispersion at  $\sim 70$  meV due to a coupling to a bosonic mode. The mode is either at much higher energies or there is a continuum which leads to the renormalization. The coupling constant as derived from the differences in the slopes of the measured dispersion and the bare particle dispersion is close to 1, independent of the dopant concentration. These values are also depicted in Fig. 3. Comparing these values with similar  $\lambda$  values at the nodal point [18] indicates that the renormalization in the normal state is rather isotropic along the Fermi surface.

To obtain further information on the renormalization of the dynamics of the charge carriers in the normal state, we have evaluated the MDC width of the *A* and the *B* bands which, multiplied by  $v_F^b$ , is a measure of the imaginary part of  $\Sigma$  plus contributions due to the finite energy and momentum resolution. Typical MDC cuts measured with a photon energy of 38 eV are shown in Fig. 4 for UD and OD samples. These cuts can be well fitted by four Lorentzians, two corresponding to the *B* and two others corresponding to the *A* band. For the OD and the UD samples the derived scattering rates at  $E_F$  are almost the same for both the *B* and the *A* bands. Values between 80 and 160 meV are derived for the antinodal point at  $T = 120$  K. These values are not far from our values ( $\sim 100$  meV) derived at the same temperature and

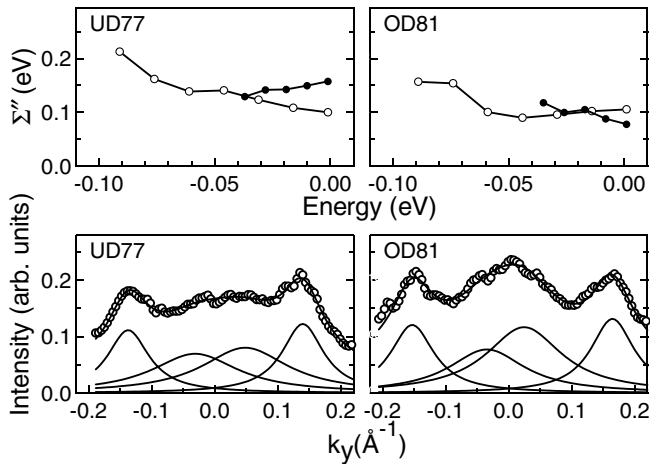


FIG. 4. Top row: imaginary part of self-energy  $\Sigma''$  as derived from MDC fits. Open (solid) symbols: bonding (antibonding) band. Bottom row: MDC fits for OD and UD samples at energies of 15 and 35 meV, respectively.

at the same energy at the nodal point. Moreover, at energies smaller than about 100 meV the scattering rates are only slightly dependent on energy (see Fig. 4). This is an indication that the modes to which the charge carriers are coupled form probably a quasicontinuous spectrum.

The results obtained can be summarized in the following way: in the normal state a rather isotropic mass renormalization of the electronic states without a clear energy scale is observed. The strength of the coupling corresponds to  $\lambda \sim 1$ . Below  $T_c$  and, in particular, in the UD samples a much higher strongly anisotropic coupling to a collective bosonic mode could be detected. We emphasize that the difference in the mass renormalization at the nodal point between the superconducting and the normal states is rather small (less than 5%).

It is difficult to interpret the entirety of our results in terms of a conventional isotropic coupling to phonons. A probably more promising model would be a coupling to spin fluctuations [19]. Although this scenario has been applied in many previous ARPES studies, the present work provides a much more detailed picture. Above  $T_c$  the system starts from charge carriers which are coupled to a continuum of spin fluctuations. The strength of the coupling is not strongly dopant dependent. Both the  $A$  and the  $B$  bands feel a similar coupling as derived from the mass renormalization and from the scattering rates. Previous ARPES studies at the  $(\pi, 0)$  point could not resolve the bilayer splitting and could not follow the flat dispersion of bands and therefore came to the conclusion that in the UD region above  $T_c$  there are only incoherent states. In the present study, renormalized dispersive and possibly coherent states are even detected above  $T_c$  in UD samples.

In the spin fluctuation scenario, below  $T_c$ , the opening of the gap leads via a feedback process to a magnetic

resonance mode at  $E_M$  detected by inelastic neutron scattering [20] to which the charge carriers couple. Because of the fact that the bilayer splitting of the band could be resolved, a quantitative analysis of the coupling strength could be performed for the  $B$  band in the entire doping range and for the  $A$  band for an UD sample. In a recent theoretical work [13] it was pointed out that according to magnetic susceptibility measurements using inelastic neutron scattering the magnetic resonance mode couples the  $A$  band only to the  $B$  band and vice versa. There is no coupling via the resonance mode within a band. It is remarkable that the coupling of the  $B$  band to the resonance mode starts when the  $A$  band just crosses the Fermi level (in the OD region). This is a further strong indication that there is a coupling to a mode only via odd susceptibilities and that the spin fluctuation scenario is applicable. Moreover, the result that in the UD region  $\lambda$  is similar for both bands is understandable, since the Fermi velocities and therefore the density of states and the odd susceptibilities  $\chi_{AB}$  and  $\chi_{BA}$  should be comparable.

This work was financially supported in part by the Schweizerische Nationalfonds zur Foerderung der Wissenschaftlichen Forschung.

- 
- [1] J. G. Bednorz and K. A. Müller, *Z. Phys. B* **64**, 189 (1986).
  - [2] P. W. Anderson, *Science* **235**, 1196 (1987).
  - [3] C. M. Varma *et al.*, *Phys. Rep.* **361**, 267 (2002).
  - [4] A. Damascelli *et al.*, *Rev. Mod. Phys.* **75**, 473 (2003).
  - [5] J. C. Campuzano *et al.*, cond-mat/0209476.
  - [6] A. Kaminski *et al.*, *Phys. Rev. Lett.* **90**, 207003 (2003).
  - [7] A. D. Gromko *et al.*, cond-mat/0202329; cond-mat/0203290205385.
  - [8] S. V. Borisenko *et al.*, *Phys. Rev. Lett.* **90**, 207001 (2003).
  - [9] J. L. Tallon *et al.*, *Phys. Rev. B* **51**, 12911 (1995).
  - [10] A. A. Kordyuk *et al.*, *Phys. Rev. Lett.* **89**, 077003 (2002).
  - [11] A. Bansil and M. Lindroos, *Phys. Rev. Lett.* **83**, 5154 (1999); J. D. Lee and A. Fujimori, *Phys. Rev. Lett.* **87**, 167008 (2001).
  - [12] Ch. Renner *et al.*, *Phys. Rev. Lett.* **80**, 149 (1998).
  - [13] M. Eschrig and M. R. Norman, *Phys. Rev. Lett.* **85**, 3261 (2000); *ibid.* **89**, 277005 (2002).
  - [14] S. Engelsberg and J. R. Schrieffer, *Phys. Rev.* **131**, 993 (1963); D. J. Scalapino, in *Superconductivity*, edited by R. D. Parks (Marcel Dekker, New York, 1969), Vol. 1, p. 449.
  - [15] A. A. Kordyuk *et al.*, *Phys. Rev. B* **67**, 064504 (2003).
  - [16] N. Nucker *et al.*, *Phys. Rev. B* **44**, 7155 (1991); V. G. Grigoryan *et al.*, *Phys. Rev. B* **60**, 1340 (1999).
  - [17] O. K. Andersen *et al.*, *J. Phys. Chem. Solids* **56**, 1573 (1995).
  - [18] A. Koitzsch *et al.*, cond-mat/0305380.
  - [19] A. V. Chubukov *et al.*, cond-mat/0201140.
  - [20] J. Rossat-Mignod *et al.* *Physica (Amsterdam)* **185-189C**, 86 (1991); H. A. Mook *et al.*, *Phys. Rev. Lett.* **70**, 3490 (1993); H. F. Fong *et al.*, *ibid.* **75**, 316 (1995).